D. Elwood
S.C. Yim

School of Civil and Construction Engineering
Oregon State University

E. Amon
A. von Jouanne
T.K.A. Brekken

School of Electrical Engineering and Computer Science

Experimental Force Characterization and Numerical Modeling of a Taut- Moored Dual-Body Wave Energy Conversion System

This paper presents an innovative modeling technique that combines experimental force measurements from a full scale linear generator with a coupled model of a two body, moored floating system to investigate the performance of a wave energy conversion system. An experiment was conducted using Oregon State University's wave energy Linear Test Bed to characterize the frictional and electromagnetic forces generated by the SeaBeavI linear generator. These force characteristics have been incorporated into the development of a coupled model using a numerical fluid-structure interaction simulation code, OrcaFlex, to predict the energy extraction potential of the system.

1 INTRODUCTION

Modern ocean wave energy research began during the oil crisis of the 1970s. Much of the early work was conducted in Europe by Salter (Salter 1976) and Evans (Evans 1979) in England and Falnes (Falnes 2002) and Budal (Budal 1977) in Norway, amongst others. Several promising concepts were developed by 1980 including point absorber wave energy converters such as the infamous Salter duck (Salter 1976) and oscillating water column (OWC) devices. Point absorbers extract energy from ocean waves by capturing the mechanical energy from the dynamic response of one or more floating bodies. If energy is extracted from a single degree of freedom (DOF) these devices can extract at most 50% of the wave energy (Evans 1979). Oscillating water column systems gather energy from the waves by converting pneumatic pressure generated by waves rising and falling in a sealed chamber into electricity. Electricity is generated by using the changing wave level to generate air flow through a nozzle driving a Wells turbine (Curran R. 1997). Early work was also conducted on the optimal control of wave energy devices (Budal 1977) (Falnes 2002). By controlling the power take-off the natural frequency of the system could be varied keeping the system in resonance with the wave forcing.

Currently, several commercial developers are working to build full scale, grid connected wave energy conversion systems. These include the Limpet (WaveGen 2008) oscillating water column, the Pelamis (Pelamis Wave Power 2008) attenuating wave energy conversion system, and the Archimedes Wave Swing (Archimedes Wave Swing 2008). In the United States, Ocean Power Technologies (Ocean Power Technologies 2008) developed a point absorber wave energy conversion buoy for the US Navy that has been tested off Oahu, Hawaii. OPT has plans to deploy an array of point absorber buoys off the coast of Reedsport, Oregon representing the first grid connected wave-energy conversion plant in the United States.

Since 2000, innovative direct-drive generator technologies have been developed for use in wave-energy conversion by the Wallace Energy Systems & Renewables Facility at Oregon State University. These direct-drive generators use electro-magnetic coupling to convert the linear motion of ocean waves into electricity. By directly coupling the relative motion between a pair of floating bodies without intermediate hydraulics or pneumatics the electrical generation efficiency can be increased and the overall system simplified.

The SeaBeavI, a 1kW direct-drive wave-energy conversion system, was designed and built by researchers at Oregon State starting in the fall of 2006 (Prudell 2007). The SeaBeavI is a taut- moored, dual-body point absorber utilizing a linear generator for power take-off (Elwood 2009). The central spar is taut-moored to the bottom and holds the armature of the linear generator. The outer taurus shaped buoy is free to heave relative to the spar creating electricity as the magnet section moves relative to the copper wires in

the armature. In October of 2007 the device was tested in the open ocean off Newport, Oregon. A rendering of the SeaBeavI is included as Figure 1.

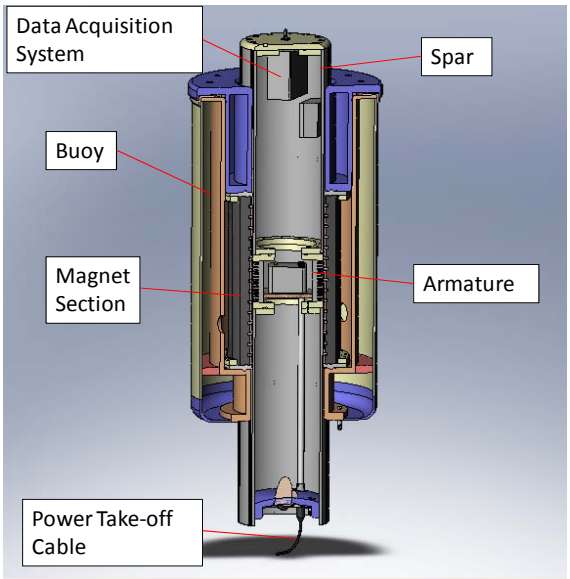

Figure 1 Rendering of spar and buoy general arrangement

2 ORCAFLEX

OrcaFlex is a coupled analysis numerical code designed to model the dynamics of offshore structures. The code has a range of capabilities from the modeling of mooring and riser systems to analysis of towed bodies and marine renewable energy systems. The coupled modeling technique used by OrcaFlex combines a finite element model of the flexible mooring and riser components with a rigid body representation of a floating system (Orcina Ltd. 2007). Hydrodynamic forces on the floating system and lines are calculated using a Morison model approach. Multiple floating bodies can be linked together using both linear and non-linear springs and dampers. A variety of wave models are available with both regular and stochastic waves.

3 PHYSICAL EXPERIMENTS

The wave energy Linear Test Bed (LTB) at the Wallace Energy Systems & Renewables Facility, shown in Figure 2, was used to test the permanent magnet linear generator to characterize the forces generated and determine the electrical efficiency of the machine. This testing provided force characteristics that were used as inputs to a coupled model of the system in OrcaFlex.

The LTB was designed and built by Mundt and Associates Inc. to evaluate direct drive wave energy conversion technologies. The test bed creates relative linear motion between the active components of the power conversion systems to simulate forces and velocities generated by a wave-energy converter. To test the permanent-magnet linear generator, the spar was fixed to a gimbaled base plate and constrained in the vertical direction. The magnet section was mounted to a gimbaled yolk coupled to a vertically translating carriage by two load cell arms. The carriage was driven by a belt-drive powered by an electric motor. This motor can be controlled via either a commanded position or force. The position of the carriage was recorded by the motor encoder and the force required to drive the carriage was measured by load cells in line with the connection between the magnet section and the carriage.

To allow for a range of sizes of devices to be tested on the LTB, three sets of load cells, each with a different maximum rating, can be used to measure the forces between device components. A set of two 22000 N load cells was installed on the load cell arms to test the SeaBeavI linear generator. The gain for the load cell signals was set by hanging a test weight from each load cell arm and measuring the voltage produced. Once the gain for each load cell had been set, the magnet section and yoke were hung from the load cell arms. The load cells were then zeroed with the weight of the yolk and magnet section as a static offset. In this way, the weight of the components was not included in the measured force recorded during data acquisition.

To characterize the forces on the linear generator the force on the system was decomposed into those forces due to friction and those due to the electrical loading on the generato:.

$$F_{Total} = F_{Frict} + F_{Gen} \quad (1)$$

where:

F_{Total} is the total measured force

F_{Frict} is the frictional force

F_{Gen} is the generator force

This allowed for the forces to be modeled separately in OrcaFlex using a combination of springs and dampers.

4 LOAD CASES

Testing of the permanent magnet linear generator was conducted in two phases. The first phase of testing focused on characterizing the frictional forces between the spar and the magnet section. These forces were measured without placing an electrical load on the

generator. In the second phase of testing, a series of fixed resistances was applied to the generator in order to measure the electromagnetic forces between the magnet section and the armature.

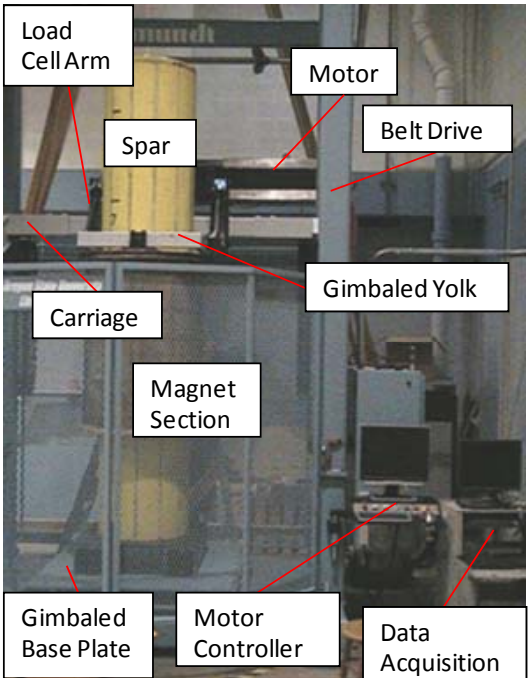

Figure 2 The active components of the permanent magnet linear generator mounted in OSU's wave energy Linear Test Bed

To characterize the frictional forces between the spar and the magnet section, a trapezoidal velocity profile was generated by the LTB. Six trials were completed with speeds ranging from .05 to .4 m/s. This low speed data allowed for the forces independent of velocity to be measured.

During trials to characterize the electromagnetic forces, the magnet section was driven with a sinusoidal velocity profile. A three-phase water rheostat was used to provide a fixed resistance for the generator. During each run, the resistance was varied to achieve a target average input power from the LTB. The voltage and current created by the generator could then be measured and the efficiency of the device calculated. The force between the magnet section and the spar was also measured to characterize the electromagnetic forces produced by the generator over a range of power levels.

For each trial, 14 channels of data were recorded with a sampling rate of 1 kHz. Data collected included: three phase voltage and current; position, velocity, and acceleration of the carriage; right load cell, left load cell and combined force from both load cells; and the input power to the LTB. For the trapezoidal velocity trials, 5 cycles at each velocity were recorded. Likewise 5 periods of data were recorded for each peak sinusoidal velocity profile.

5 CHARACTERIAZATION OF FRICTIONAL FORCES

The frictional forces between the spar and the buoy can be decomposed into the mechanical contact friction, the fluid shear forces due to the small gap between the buoy and the spar, and the electro-magnetic force between the generator components in the no-load condition:

$$F_{Frict} = F_C + F_F + F_{EM} \tag{2}$$

where:

F_C is the contact friction force

F_F is the fluid shear force

F_{EM} is the no load electro-magnetic force

If the contact friction force is assumed to be Coulomb friction then the force can be expressed as a function of the normal force between the two bodies and the coefficient of friction of the bearing material:

$$F_C = \mu N \tag{3}$$

where:

μ is the coefficient of friction

N is the normal force

The electro-magnetic force between the buoy and spar in the no load condition is due to the core losses of the machine. The core loss is the sum of the magnetic hysteresis losses and the eddy current losses in the generator laminations (El-Hawary 1986):

$$F_{EM} = F_h + F_E \tag{4}$$

where:

F_h is the force due to magnetic hysteresis

F_E is the force due to eddy currents

The force due to the hysteresis is a function of the maximum magnetic flux density, the pole pitch, and the material properties of the magnets (El-Hawary 1986):

$$F_h = k_h \frac{1}{P} (B_m)^n \tag{5}$$

where:

B_m is the maximum flux density

P is the pole pitch of the armature

k_h is a constant of the material

n is determined from experiments and ranges from 1.5 to 2.5

The eddy current forces are also dependant on the maximum flux density, pole pitch and the material properties of the magnets. In addition the eddy current forces are also a function of the velocity of the generator and thickness of the generator laminations (El-Hawary 1986):

$$F_e = k_e \frac{V}{P}(B_m t)^2 \quad (6)$$

where:

V is the generator velocity

k_e is an empirical constant

t is the thickness of the generator laminations

The force data from the trapezoidal velocity trials on the LTB was analyzed to determine the dry sliding friction and no-load electromagnetic force between the buoy and the spar. For each of the 5 cycles, the measured force was averaged over the constant velocity section. This averaging filtered out the magnetic cogging forces generated as each magnet passed between poles of the armature. Cogging is a conservative force that is generated by the gap between pole tips. As such it is not considered to be a frictional force and is neglected here.

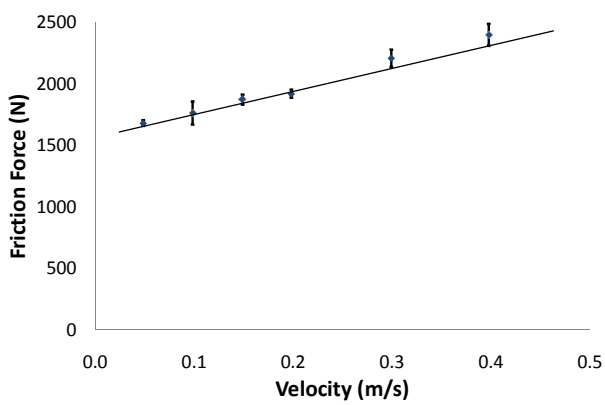

Figure 3 Average measured force between the magnet section and the spar as a function of velocity

Once the force data was filtered for each of the 5 cycles of each trapezoidal velocity, the average of all of the cycles was calculated. The error in the measurement was assumed to be 2 times the standard deviations of the 5 samples and ranged from +-23 N to +-93 N. As can be seen in Figure 3, the force increased with increasing velocity from just less than 1700 N at .05 m/s to slightly more than 2400 N at .4 m/s. The zero speed force offset is believed to be the sum of the contact friction force and the hysteresis force. The velocity dependant portion of the measured force is likely due to eddy current losses which are directly proportional to the generator velocity.

The measured force on the linear test bed was much greater than expected given the low friction material used to construct the linear bearings. The manufacturer-supplied friction coefficient for the bearing material is .1, and the theoretical normal force between the magnet section and the spar due to the magnetic forces is zero; assuming the spar is perfectly centered inside the magnet section. If the spar and magnet section are not perfectly concentric, however, the normal force between the magnets and the armature can become very large, potentially resulting in the higher than expected frictional force.

To enable effective magnetic force transmission between the buoy and the spar the gap between the two floating bodies was only 5mm. A commercial computational fluid dynamics code, StarCCM+ (CD-Adapco 2008), was used to estimate the hydrodynamic force due to the small gap between the spar and buoy.

A two-dimensional, laminar flow model was created in StarCCM+ to estimate the shear stresses on the outer wall of the spar and the inner surface of the magnet section. The governing equations for the model were the continuity equation and the Navier-Stokes equations for the x and y momentum. The solution domain was bounded by a fixed wall, an oscillating, a stagnation inlet, and a pressure outlet as seen in Figure 4. The pressure at the inlet and outlet of the domain was defined using linear wave theory as the pressure field under a monochromatic progressive wave at z=x=0:

$$P_{Inlet} = \rho g \frac{H}{2} \cos(\sigma t) \quad (7)$$

$$P_{Outlet} = -\rho g * (.15) + \rho g \frac{H}{2} \cos(\sigma t) \quad (8)$$

where:

ρ is the fluid density

g is the gravitational acceleration

H is the wave height

σ is the wave frequency

t is time

A no slip boundary condition was imposed on the fixed wall on the left side of the domain. The velocity of the oscillating wall was:

$$V_{wall} = \frac{H}{2}\sigma\cos(\sigma t) \quad (9)$$

This velocity assumes that the buoy is a perfect wave follower. The length of the solution domain was set to .15 m for computational efficiency.

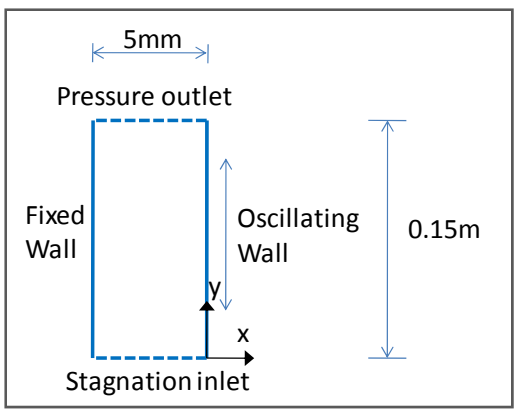

Figure 4 Solution domain defined in StarCCM+ to estimate the shear stress in the gap between the buoy and the spar

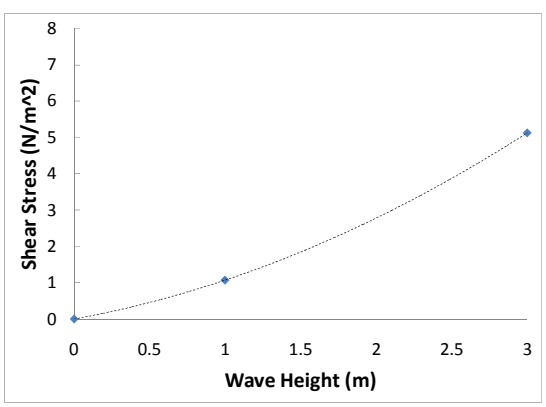

Figure 5 Shear stress on the oscillating wall as a function of the wave height

The shear maximum shear stress in the gap was estimated for two wave heights and two gap widths. As can be seen in Figure 5 the shear stress in the gap was proportional to the wave height squared. The shear stress was independent of the gap width over the range of gap widths investigated. With the as built gap of 5mm the maximum shear stress on the oscillating wall was 5.1 N/m^2 corresponding to a total fluid shear force of 28.9 N. This fluid shear force is approximately 1.3% of the maximum force measured during the LTB experiments. The CFD results indicate that the fluid shear force in the gap between the spar and buoy is negligible when compared with the other frictional forces acting on the system. Further testing of the system in water is still required to validate these results.

6 CHARACTERIAZATION OF ELECTROMAGNETIC FORCES

The force data from sinusoidal velocity trials was used to characterize the electromagnetic force created by the generator while under load. For each peak speed, the fixed resistance was adjusted until the LTB input power reached the desired level. At each of the 5 peak velocities, the generator was run with a series of fixed resistances. The force data from each of these trials was processed using Matlab and the frictional force was subtracted from the total force. This allowed the relationship between electromagnetic force and velocity to be determined using a graphical approach. As can be seen in Figure 6, the relationship between force and velocity shows a force ripple due to the magnetic cogging generated as the permanent magnets passed by the poles of the armature.

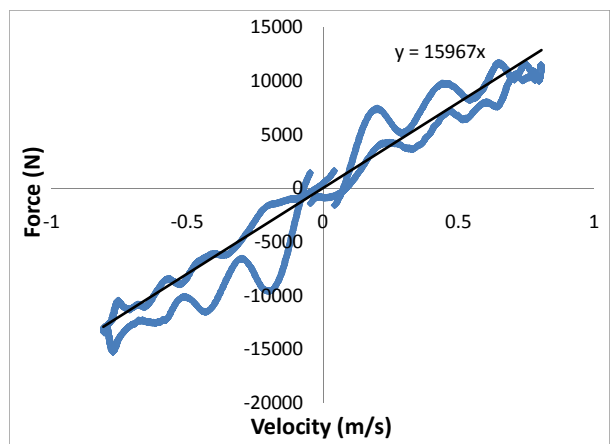

Figure 6 Relationship between force and velocity, .8 m/s peak sinusoidal velocity, 14.13 Ohm fixed resistance

Having established a linear relationship between electro-magnetic force and velocity over a range of fixed resistances, the generator force can be represented as a velocity dependent damping. The

linearized damping can be expressed as a function of the fixed resistance to create a force characteristic for the linear generator. This force characteristic can be seen in Figure 7. The generator damping shows an inverse power relationship when plotted against the fixed resistance. Theory predicts that the exponent in this case should be -1. The deviation of the measured data from the theory may be due to the impedance of the linear generator.

The electromagnetic forces produced by the linear generator were larger than was anticipated. At its rated speed, the generator was able to produce approximately 5 times more power as was originally intended. Increased capacity led to larger forces under load, therefore the buoy and spar, as designed, were insufficient to drive the linear generator.

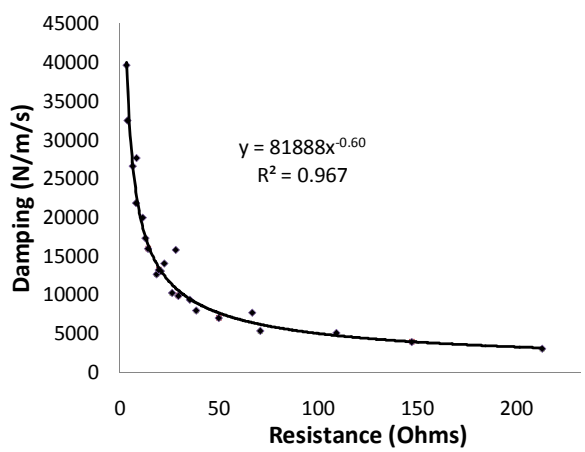

Figure 7 Linear generator damping coefficient as a function of the fixed resistance

7 SYSTEM CONFIGURATION

Initially, the as-built configuration of the SeaBeavI wave energy conversion system was modeled in OrcaFlex to investigate the performance of the system. It was quickly determined that the waterplane stiffness of the buoy was insufficient to provide the force required to drive the linear generator.

Additionally, the excess buoyancy of the spar was not great enough to keep the mooring in tension during the down stroke of the buoy. The diameter of the buoy was increased, adding hydrostatic stiffness, and a circular footing was added to the spar in order to increase the pre-tension in the mooring. The geometry of the resized SeaBeavI is shown in Figure 8.

The mooring system connecting the spar to the ocean floor is a single tensioned leg composed of chain, spectra rope, and a mid-column float. The mooring used in the OrcaFlex model was made to accurately represent the as-designed mooring for the SeaBeavI wave energy conversion system.

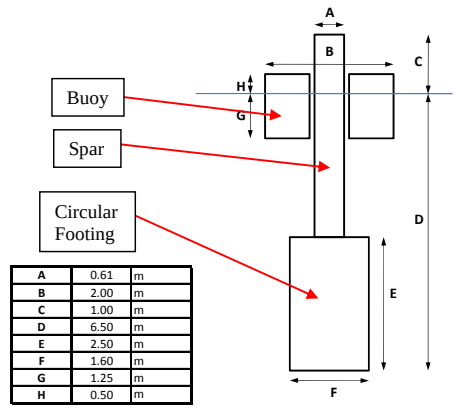

A	0.61	m
B	2.00	m
C	1.00	m
D	6.50	m
E	2.50	m
F	1.60	m
G	1.25	m
H	0.50	m

Figure 8 Geometry of the resized SeaBeavI

8 LINEAR GENERATOR MODEL

To model the forces applied to the system by the linear generator, a linear damper was used to connect the spar and buoy in OrcaFlex. The damper exerts a force on the spar proportional to the relative velocity between the two floating bodies using the damping coefficients measured during the testing of the SeaBeavI linear generator. By using a linear damper, the generator model in OrcaFlex represents the generator running with a fixed resistive load. A generator using either current or voltage control could also be modeled using the combination of a non-linear spring and a non-linear damper in place of the linear damper. The damper used to model the linear generator can be seen in Figure 9.

9 CONTACT/FRICTION MODEL

The contact forces and friction between the spar and the buoy were modeled using four linear springs and a non-linear damper. Four linear springs were used to model the horizontal contact force between the bearing strips on the spar and the stainless steel tube on the buoy.

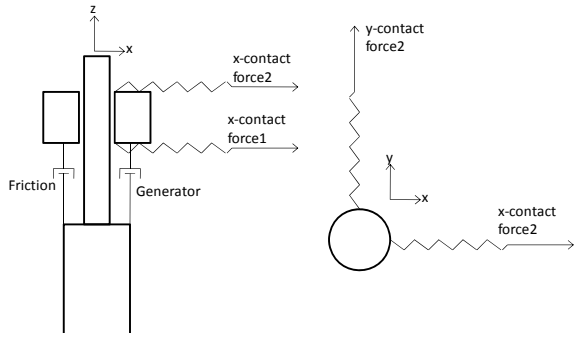

Figure 9 Springs and Dampers used to model the contact forces, friction, and generator force between the buoy and the spar

Two springs at the top of the buoy provided restraint in the x and y-directions with two similar springs at the bottom of the buoy. The springs were made to be very long and very stiff in order to provide horizontal restoring force without introducing any vertical forces. The springs used to model the contact force between the buoy and the spar can be seen in Figure 9.

The friction force between the buoy and the spar was modeled using a non-linear damper. The relationship between the force and the velocity in the non-linear damper was determined using the data collected from the Linear Test Bed. The shape of the friction characteristic is shown in Figure 10. The friction modeled using the non-linear damper is essentially coulomb friction except that the force is slightly velocity dependant due to electromagnetic effects.

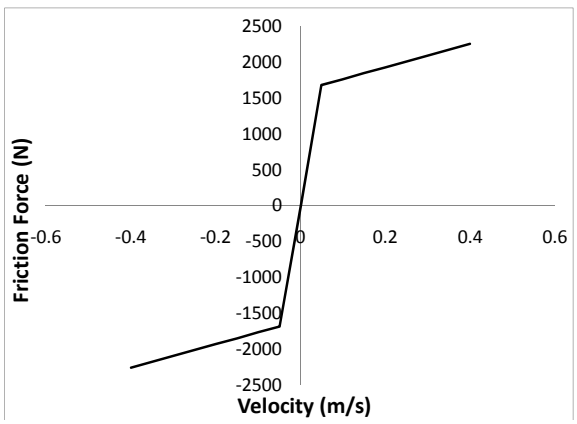

Figure 10 Characteristic of the non-linear damper used to model the friction between the buoy and the spar

10 LOAD CASES

The system's performance was investigated in regular waves in order to determine the effect of the generator forces on the performance of the system. Load cases included wave periods ranging from 4 to 9 seconds with wave heights from 0.5 to 2 meters. Those cases with steepness greater than 1/7 were not run since the waves would transition to breaking at this point and the wave theory employed would no longer be valid. For each wave height and period the linear damping coefficient of the generator was iterated until the damping value producing maximum mechanical power was found.

11 NUMERICAL RESULTS

An optimal value for the generator damping was found for each wave height and period. As can be seen in Figure 11, the power output versus damping has a clear maximum around 20 kN/(m/s). The shape of the power curve was consistent for all of the load cases investigated. The optimal generator damping decreased with increasing wave height as illustrated by Figure 12. There was an inverse relationship between the wave period and the optimal damping.

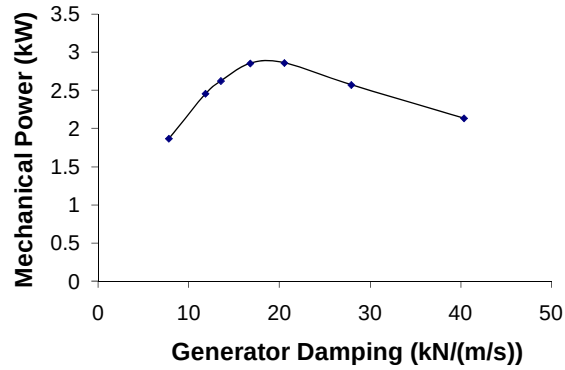

Figure 11 Relationship between generator damping and input generator power in a 2m, 8 second wave

The mechanical power produced by the system in regular waves increases linearly with increasing wave height. As the period of the wave is decreased at a given wave height the mechanical power increases up to the resonant frequency of the buoy as can be seen in Figure 13.

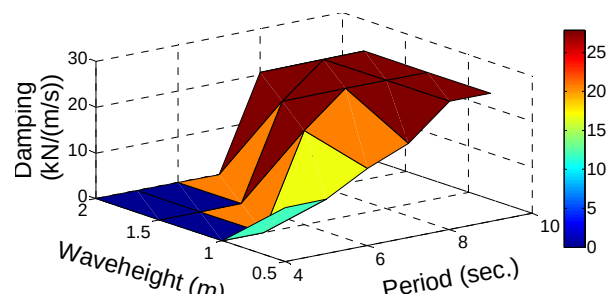

Figure 12 Relationship between the wave period, wave height, and optimal damping for the regular wave load cases

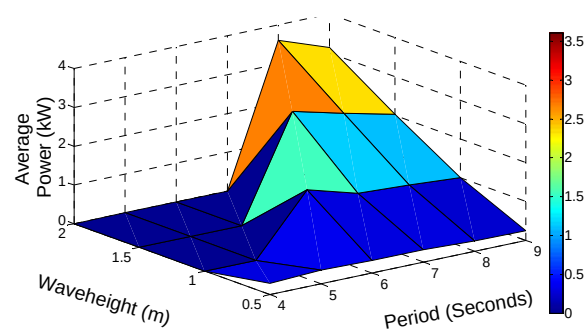

Figure 13 Average mechanical power produced in regular waves

12 CONCULSIONS AND FUTURE WORK

In this paper a method for modeling power take-off forces on a wave-energy conversion system by integrating data from physical experiments into a coupled numerical model has been presented. This model has been used to determine the effect of generator and frictional forces on the dynamics of a two body floating system and estimate the optimal damping and power output in regular waves.

The forces measured on the Linear Test Bed were decomposed into the frictional forces on the system and the forces due to electrical load on the generator. The frictional forces were further decomposed into contact friction force, no load electro-magnetic force, and a fluid shear force. The contact friction and no load electro-magnetic forces were measured on the LTB. The force due to the fluid shear stress was estimated using computational fluid dynamics and was found to be negligible compared to the other frictional forces.

Future work to determine the frictional coefficients of bearing materials operating in sea water and the normal forces on the system will help to refine contact friction model. Experiments to measure the frictional forces in waves are also required to verify the predictions of the CFD analysis.

AKNOWLEDGEMENTS

This project would not have been possible without support from the Department of Energy and our industry partner Columbia Power Technologies. The second author also acknowledges partial financial support from the Office of Naval Research Grant Nos. N00014-04-10008 and N0014-07-10207.

REFERENCES

Archimedes Wave Swing. 6 June 2008 <http://awsocean.com/>.

Budal, K. "Theory for absorption of wave power by a system of interacting bodies." Journal of Ship Research (1977): 248-253.

CD-Adapco. STAR-CCM+. July 2008 <http://www.cd-adapco.com/products/STAR-CCM_plus/>.

Curran R., L.M.C Gato. "The energy conversion performance of several types of Wells turbine designs." Proceedings of the Institute of Mechnical Engineers (1997): 133-145.

Dean, Robert G., Darlrymple R.A. Water Wave Mechanics for Engineers and Scientists. Hackensack, NJ: World Scientific, 1991.

El-Hawary, Mohamed E. Principles of Electric Machines with Power Electronic Applications. Englewood Cliffs, NJ: Prentice-Hall, 1986.

Elwood, D., J. Prudell, C. Stillinger, A. Brown, A. von Jouanne, T. Brekken, Robert Pasch. "Design, Construction, and Ocean Testing of a Taut-Moored Dual-Body Wave Energy Converter with a Linear Generator Power Take-off." Proceedings of the 28th Annual Conferance on Offshore Mechanics and Arctic Engineering. Honolulu, Hawaii: ASME, (Submitted).

Evans, D.V. "Some theoretical aspects of three dimensional wave energy absorbers." Proceedings of the First Symposium on Wave Energy Utilization. Gothnburg, Sweden: Chalmers University of Technology, 1979. 77-106.

Falnes, J. Ocean Waves and Oscillating Systems. Cambridge, UK: Cambridge University Press, 2002.

Ocean Power Technologies. Ocean Power Technologies. 6 June 2008 <http://www.oceanpowertechnologies.com/>.

Orcina Ltd. "OrcaFlex Manual." Daltongate, UK: Orcina Ltd. (2006)

Pelamis Wave Power. Pelamis Wave Power. 6 June 2008 <http://www.pelamiswave.com>.

Prudell, J.H. "Novel design and implementation of a permanant magnet linear tubular generator for wave energy conversion." Masters Thesis. Corvallis, OR: Oregon State University, 2007.

Salter S.H., D.C. Jeffery, J.R.M. Taylor. "The architecture of nodding duck wave power generators." The Naval Architect (1976).

WaveGen. WaveGen. 6 June 2008 <http://www/wavegen.co.uk>.